The Astrophysical Journal Letters, 728:L26 (5pp), 2011 February 20 doi:10.1088/2041-8205/728/2/L26

THE FAINT END OF THE QUASAR LUMINOSITY FUNCTION AT $z \sim 4$: IMPLICATIONS FOR IONIZATION OF THE INTERGALACTIC MEDIUM AND COSMIC DOWNSIZING*

Eilat Glikman[1,5], S. G. Djorgovski[2], Daniel Stern[3], Arjun Dey[4], Buell T. Jannuzi[4], and Kyoung-Soo Lee[1,6]
[1] Department of Physics and Yale Center for Astronomy and Astrophysics, Yale University, P.O. Box 208121, New Haven, CT 06520-8121, USA; eilat.glikman@yale.edu
[2] Astronomy Department, California Institute of Technology, Pasadena, CA 91125, USA
[3] Jet Propulsion Laboratory, California Institute of Technology, Pasadena, CA 91109, USA
[4] National Optical Astronomy Observatory, 950 N. Cherry Ave., Tucson, AZ 85719, USA
Received 2010 November 15; accepted 2010 December 22; published 2011 January 25

ABSTRACT

We present an updated determination of the $z \sim 4$ QSO luminosity function (QLF), improving the quality of the determination of the faint end of the QLF presented by Glikman et al. (2010). We have observed an additional 43 candidates from our survey sample, yielding one additional QSO at $z = 4.23$ and increasing the completeness of our spectroscopic follow-up to 48% for candidates brighter than $R = 24$ over our survey area of 3.76 deg^2. We study the effect of using K-corrections to compute the rest-frame absolute magnitude at 1450 Å compared with measuring M_{1450} directly from the object spectra. We find a luminosity-dependent bias: template-based K-corrections overestimate the luminosity of low-luminosity QSOs, likely due to their reliance on templates derived from higher luminosity QSOs. Combining our sample with bright quasars from the Sloan Digital Sky Survey and using spectrum-based M_{1450} for all the quasars, we fit a double power law to the binned QLF. Our best fit has a bright-end slope, $\alpha = 3.3 \pm 0.2$, and faint-end slope, $\beta = 1.6^{+0.8}_{-0.6}$. Our new data revise the faint-end slope of the QLF down to flatter values similar to those measured at $z \sim 3$. The break luminosity, though poorly constrained, is at $M^* = -24.1^{+0.7}_{-1.9}$, approximately 1–1.5 mag fainter than at $z \sim 3$. This QLF implies that QSOs account for about half the radiation needed to ionize the intergalactic medium at these redshifts.

Key words: cosmology: observations – galaxies: luminosity function, mass function – large-scale structure of universe – quasars: general – surveys

Online-only material: color figure

1. INTRODUCTION

The primary observable that traces the evolution of QSO populations is the QSO luminosity function (QLF) as a function of redshift. The QLF can be well represented by a broken power law: $\Phi(L) = \phi^*[(L/L^*)^\alpha + (L/L^*)^\beta]^{-1}$, where L^* is the break luminosity. Current measurements poorly constrain the corresponding break absolute magnitude to be $M^*_{1450} \simeq -25$ to -26 mag, at $\lambda_{\rm rest} = 1450$ Å. The bright-end slope, α, appears to evolve and flatten toward high redshifts, beyond $z \sim 2.5$ (Richards et al. 2006). The faint-end slope, β, has been measured to be around -1.7 at $z \lesssim 2.1$; it is poorly constrained at higher redshifts, but appears to flatten at $z \sim 3$ (Hunt et al. 2004; Siana et al. 2008). At yet higher redshifts, the situation is much less clear due to the relatively shallow flux limits of most surveys to date (e.g., Wolf et al. 2003; Richards et al. 2006). The shape of the QLF at $z > 3$ is still not well measured, and the evolution of L^* and the faint-end slope remain poorly constrained.

We recently measured the faint end of the QLF at $z \sim 4$ and found an unexpected result: the QLF appeared to rise steeply toward faint luminosities, steeper than at lower redshifts, and in apparent conflict with some theoretical models (Glikman et al. 2010, hereafter Paper I). This implied a more complex co-evolution of active galactic nuclei (AGNs) and galaxies in the first 2 Gyr of the universe, and suggested that AGNs are a more significant contributor to the metagalactic ionizing UV flux than previously estimated. However, the faint-end slope computed in Paper I relied on the faintest bin, which was highly incomplete with only two QSOs confirmed. Recently, Ikeda et al. (2011) measured the faint end of the QLF from $z \sim 4$ QSOs in the COSMOS field and found a lower space density by a factor of ~3–4 and a flatter slope. The COSMOS survey covers a 43% smaller area than our survey and has three times fewer QSOs (8 versus 24). In this Letter, we present new spectroscopic observations from our survey which increase our completeness and yield an improved estimate of the $z \sim 4$ QLF down to $M_{1450} = -21$ mag, primarily due to our improved determination of the contamination rates in the lowest luminosity bin used to compute the QLF.

We use standard cosmological parameters throughout the Letter: $H_0 = 70\,{\rm km\,s^{-1}\,Mpc^{-1}}$, $\Omega_M = 0.30$, and $\Omega_\Lambda = 0.70$.

2. SAMPLE SELECTION AND PREVIOUS RESULTS

We directly measured the $z = 4$ QLF by taking advantage of two publicly available, deep, multiwavelength imaging surveys. The selection methodology is described in detail in Paper I. Our QSO sample is derived from the NOAO Deep Wide-Field Survey (NDWFS; Jannuzi & Dey 1999) and the Deep Lens Survey (DLS; Wittman et al. 2002), which reach magnitude limits of $R \gtrsim 24$ and provide multiwavelength imaging in B, V, R, I, and z, depending on the survey. We selected subfields from these surveys amounting to a total area of 3.76 deg^2 (1.71 deg^2 in NDWFS and 2.05 deg^2 in DLS). We created source catalogs

* The data presented herein were obtained at the W. M. Keck Observatory, which is operated as a scientific partnership among the California Institute of Technology, the University of California and the National Aeronautics and Space Administration. The Observatory was made possible by the generous financial support of the W. M. Keck Foundation.
[5] NSF Astronomy and Astrophysics Postdoctoral Fellow.
[6] Jaylee and Gilbert Mead Fellow.

from these images using SExtractor (Bertin & Arnouts 1996) in dual-image mode, requiring a detection in the R band.

To derive and understand our selection function, we built a library of model QSO spectra spanning the redshift range $3.5 < z < 5.2$, including Monte Carlo realizations of Lyα forest absorbers along the line-of-sight, continuum slope, and Lyα equivalent width, to determine the location of these QSOs in color–color space. We applied color cuts to our catalogs, resulting in 148 QSO candidates, 30 of which are brighter than $R = 23$. In Paper I we reported 28 spectra, concentrating on the brightest sources, of which 23 were QSOs with $3.74 < z < 5.06$. Twenty of these are brighter than $R = 23$. Interestingly, two QSOs at $z \sim 4$ had anomalous N IV] 1486 Å emission, suggesting the presence of very massive, metal-poor star formation in their hosts (i.e., Population III; Glikman et al. 2007).

We used the modeled QSO spectra to compute the selection probability of a QSO in our survey as a function of R magnitude and redshift. This allowed us to compute the volume density of quasars as a function of luminosity, $\Phi(M_{1450}, z = 4)$, using the $1/V_a$ method (Page & Carrera 2000).

We computed the QLF at a fiducial wavelength that, for high-redshift, optically selected QSOs, is 1450 Å. This wavelength lies in a part of the rest-frame ultraviolet that is free from emission lines and is a proxy for the continuum luminosity. Lower redshift surveys typically derive the QLF at rest-frame B band (e.g., Pei 1995; Croom et al. 2004), while Richards et al. (2006) use the absolute magnitude of a $z = 2$ quasar in the i band, $M_i(z = 2)$, for the Sloan Digital Sky Survey (SDSS) QLF.

A standard way to convert an observed magnitude to a monochromatic rest-frame absolute magnitude at 1450 Å is to add an appropriate K-correction, which is often computed either from a QSO template or simulated QSOs, such as our library of model QSO spectra (see Paper I). At low redshifts, optical spectra do not cover rest-frame 1450 Å, and K-corrections are the only option. However, if rest-frame 1450 Å is covered by the spectrum of a quasar, a more direct way to compute M_{1450} is to convolve a spectrum that has been shifted to the rest frame with a top hat filter centered at 1450 Å and apply a distance modulus. To account for slit losses, we convolve our spectra with a photometric filter (I or z, depending on the survey) and scale the fluxes to the image-based photometry. In Paper I we measured M_{1450} for our QSOs using both methods: directly from the spectra and by applying a K-correction determined from our simulated model spectra. We found that M_{1450} measured directly from the spectra were ∼0.3 mag fainter, on average, than M_{1450} computed with K-corrections.

In Paper I our spectroscopic completeness for $R < 23$ was 73% and we computed the QLF using only these brightest QSOs. We found that regardless of the method for computing M_{1450}, the faint-end slope of the QLF was steeper than at lower redshifts when fit by a single power law, $\Phi(M) = \Phi^* 10^{-0.4(\beta-1)M}$. The best-fit slopes were $\beta = -1.6 \pm 0.2$ and $\beta = -1.2 \pm 0.2$ for the K-correction-based and spectrum-based M_{1450}, respectively. Once we added the three QSOs with $R > 23$ (whose spectroscopic completeness was only 5%), the QLF became even steeper with $\beta = -2.0 \pm 0.2$ and $\beta = -2.5 \pm 0.2$, for the K-correction-based and spectrum-based M_{1450}, respectively.

These steep slopes persisted when we combined the faint QSOs with the QLF derived from SDSS quasars in Richards et al. (2006) and Fontanot et al. (2007) and a double power-law fit to the combination of the bright-end QLF from Richards et al. (2006) and the faint-end points based on spectrum-based M_{1450} yielded a bright-end slope, $\alpha = -2.4 \pm 0.2$, and faint-end slope, $\beta = -2.3 \pm 0.2$, without a well-constrained break luminosity; this was effectively a single power law.

There were two immediate cosmological implications to this result: (1) models of the evolution of faint AGNs at ∼1 Gyr after the end of the reionization, and possibly all the way into the reionization era, would need to be revised; and (2) AGNs were a more significant contributor to the metagalactic ionizing UV flux at these epochs, affecting the evolution of the intergalactic medium (IGM; Haiman et al. 2001; Wyithe & Loeb 2003; Shankar & Mathur 2007). However, as emphasized in Paper I, these results were based on only a few QSOs in the faintest bin, $23 < R < 24$.

3. ADDITIONAL SPECTROSCOPY

We sought to improve the measurement of the faint-end slope by obtaining additional spectra of $R > 23$ candidates. On UT 2010 May 17–18, we obtained 38 additional spectra with LRIS on Keck I. To maximize our efficiency, we observed using slit masks selecting candidates that lay within a single slit mask ($4' \times 8'$). We observed 22 candidates in NDWFS, 19 of which were fainter than $R = 23$ magnitudes. We observed 16 DLS candidates, all fainter than $R = 23$. In addition, we obtained five spectra with DEIMOS on UT 2010 May 14 of NDWFS candidates as part of an observing program studying $z \sim 4$ Lyman break galaxies (LBGs) in the Boötes field (Lee et al. 2010).

Even though we increased our spectroscopic completeness by more than a factor of two, only one $z = 4.23$ QSO ($R = 23.20$) was found in the NDWFS field. No QSOs were found in the DLS field. In Figure 1, we show the R-magnitude distribution of our candidates. On top we show the distribution of candidates with spectra from Paper I in solid bins and the newly obtained spectra in shaded bins. The bottom panel shows the efficiency of finding QSOs as a function of magnitude. It is clear that our selection efficiency drops significantly beyond $R = 23$.

The spectra that were not classified as QSOs fell into three categories: (1) featureless, unidentifiable spectra, (2) LBGs at similar redshifts ($z \sim 3$–4), and (3) carbon stars. The objects with featureless spectra are not QSOs because they have smooth continua to the shortest wavelength end of the LRIS red camera ($\lambda \gtrsim 5600$ Å) and no lines were identified. The typical rms of our spectra is $\sim 10^{-19}$ erg s^{-1} cm^{-2} Å^{-1}, and the faintest Lyα lines in our survey has a peak flux density of $\sim 4 \times 10^{-18}$ erg s^{-1} cm^{-2} Å^{-1}. With a signal-to-noise ratio of $\gtrsim$10, Lyα has an unmistakeable signature in these spectra and its absence virtually guarantees that the object is not a QSO.

LBGs at the same redshifts as the QSOs in our survey are a natural contaminant since their spectra also show the strong spectral break at ∼6000 Å due to absorption by the Lyα forest. As we probe fainter fluxes we intersect the bright end of the LBG luminosity function. Steidel et al. (1999), using a somewhat different color selection at $z \sim 4$, estimated a surface density of ∼15 LBGs per deg^2 down to $I_{AB} \simeq 23.5$ mag and ∼65 LBGs per deg^2 down to $I_{AB} \simeq 24$ mag. This amounts to 56 and 244 LBGs expected in our area for the two magnitude limits, respectively, which is roughly consistent with the number of interlopers in our faintest bins.

Carbon stars are common interlopers in high-redshift QSO surveys (Richards et al. 2002) and vice versa (Downes et al. 2004). A more detailed discussion of our spectroscopic results will be presented in an upcoming paper.

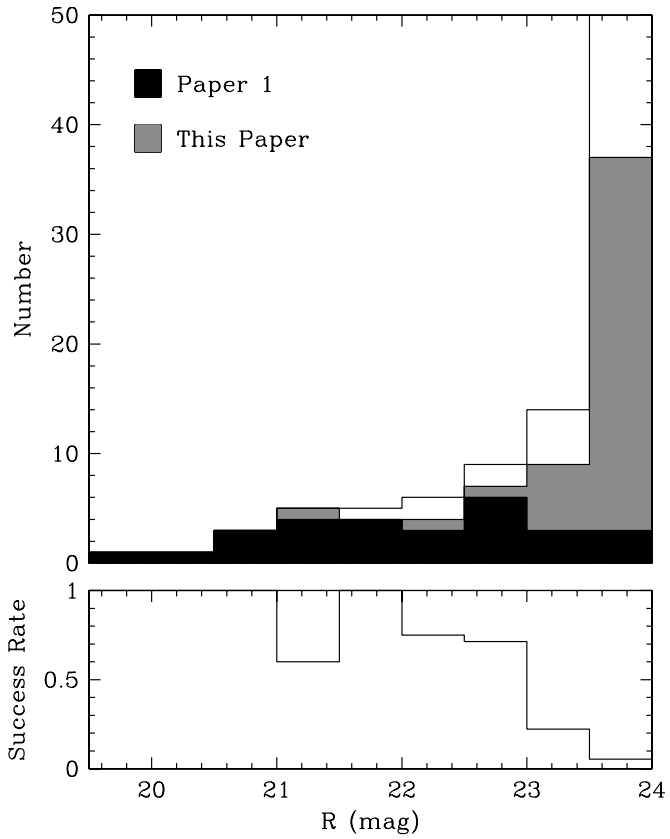

Figure 1. We have improved the completeness of our spectroscopic follow-up of our QSO candidates since Paper I. Top: *R*-magnitude distribution of our quasar candidates. Overplotted are objects with spectra from Paper I (solid) and this work (shaded, additional objects observed 2010 May). Bottom: efficiency of the spectroscopic sample as a function of *R*-band magnitude. Note that our efficiency drops significantly for $R > 23$.

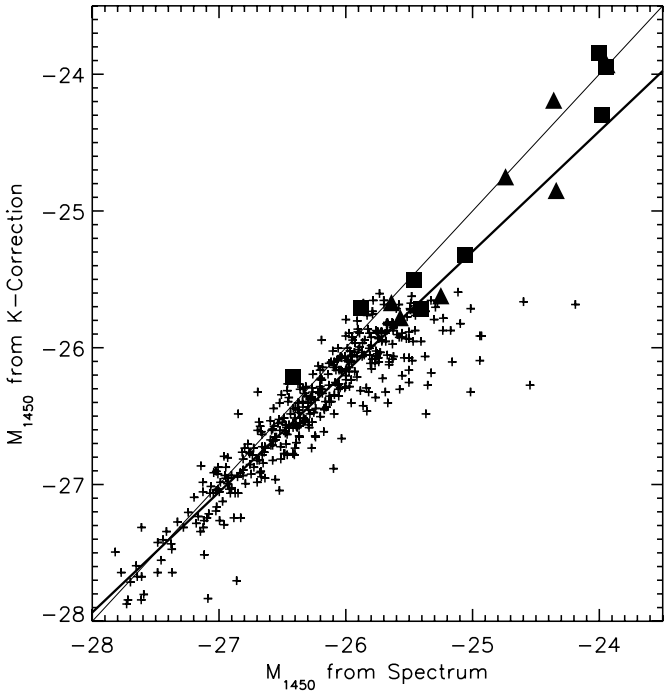

Figure 2. *K*-corrected absolute magnitudes at rest-frame 1450 Å vs. the M_{1450} measured directly from the QSO spectra. The SDSS QSOs are represented with plus signs, squares are DLS QSOs, and triangles are QSOs from NDWFS. The thick line is the best-fit relationship to all the points, with a slope of 0.9 and an offset of −3.3. The thin line shows a one-to-one relation. M_{1450} measured from spectrophotometry are significantly fainter (particularly at lower luminosities) than those derived from *K*-corrections. This may be because the QSO templates used were derived from high-luminosity objects, yet are applied to the full range of source luminosities in our sample.

4. RESULTS

In Paper I we presented two versions of the QLF using absolute magnitudes computed from *K*-corrections as well as directly from the spectra. Since the *K*-corrections rely on a QSO template, distribution of UV continuum slopes, and distribution of Lyα equivalent widths, the latter two of which are modeled as Gaussian distributions, the luminosity derived from these *K*-corrections is heavily dependent on assumptions about the spectral properties of QSOs. The measurement of M_{1450} from spectrophotometry more directly reflects the true luminosity of each QSO. Therefore, going forward we only use M_{1450} measured from spectroscopy.

We extend our QLF to higher luminosities using QSOs from SDSS. In Paper I we compared our faint-end QLF with the SDSS-based QLF from Richards et al. (2006) and Fontanot et al. (2007). Although both bright-end QLFs used the same QSOs from SDSS, they derived volume densities that differed by more than a factor of two at their faintest bins. This was due to different methods of deriving the selection function. Fontanot et al. (2007) used the QSO template from Cristiani & Vio (1990) and line and continuum properties based on the SDSS spectroscopic sample itself. Richards et al. (2006), using a method more similar to ours, built a library of model QSO spectra with Gaussian distributions of line and continuum properties as we have done. Therefore, to construct a QLF that will consistently span the full range of luminosities, we use the selection function derived by Richards et al. (2006) except that we re-compute M_{1450} for the SDSS QSOs directly from their spectra.

We identified QSOs from Richards et al. (2006, Table 5) with $3.8 < z < 5.2$ to match the redshift range of our QSO selection; 399 QSOs were selected. We obtained their spectra from the SDSS database and measured M_{1450} from each spectrum directly in the same manner as done for our faint QSOs. Figure 2 compares M_{1450} from *K*-corrected magnitudes (using Equation (3) from Richards et al. 2006) with the spectrophotometrically derived values. We include our faint QSOs as squares (DLS) and triangles (NDWFS). We find that measuring M_{1450} from *K*-corrections introduces a bias that overestimates the luminosities of QSOs. The effect appears to be more pronounced at fainter luminosities. This may be because the QSO template used to derive *K*-corrections is composed of luminous QSOs. Luminous QSOs have more prominent blue bumps and therefore have stronger rest-frame UV emission than lower luminosity QSOs. Fainter objects have weaker blue bumps and may be overcorrected by the *K*-correction technique, resulting in the bias seen in Figure 2.

We use these new absolute magnitudes to compute $\Phi(M)$ using the value of the selection function from Table 5 of Richards et al. (2006) and computing the available volume for each quasar, V_a, with the limiting magnitude of $i = 20.2$. We bin the QLF in one-magnitude bins and find that the faint end of the SDSS QLF matches quite well with the bright end of our survey (Figure 3). Note that the faintest bin of the SDSS QLF is an outlier, likely due to incompleteness. The open red circles show the QSO volume density derived in Paper I. Table 1 lists the

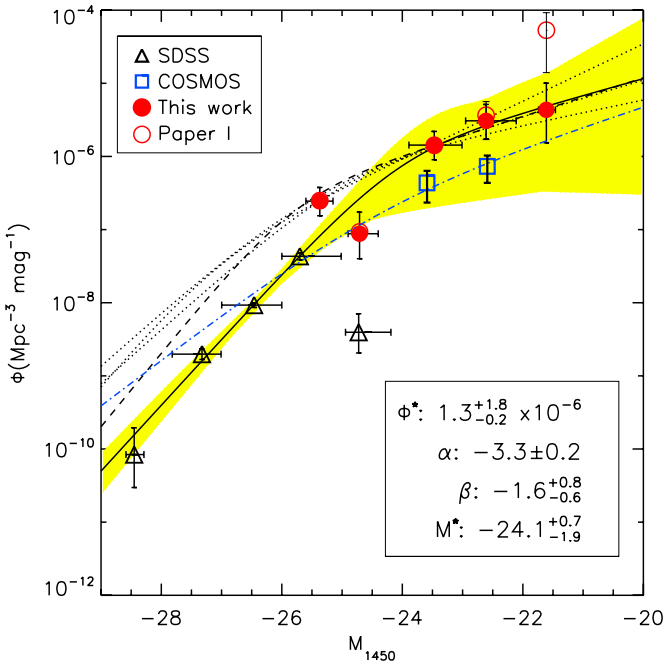

Figure 3. QSO luminosity function at $z \sim 4$, combining the QLF from SDSS (triangles) and our new, updated data (filled red circles). The points are plotted at the mean luminosity of each bin. We overplot the QLF from Paper I with open red circles, to show the change with increased spectroscopic completeness. The blue squares are the space densities of $z \sim 4$ QSOs from Ikeda et al. (2011) and the dot-dashed line is their best-fit double power law. The lower right-hand legend lists the best-fit parameters to a double power-law (solid line) shaded region represents the 1σ uncertainties. Dashed and dotted lines show the $z \sim 3$ QLF from Siana et al. (2008), representing the different fits to their QLF. While the faint-end slopes agree with our measurements, our normalization, Φ^*, is higher than Ikeda et al. (2011) by a factor of ∼4.

(A color version of this figure is available in the online journal.)

Table 1
Luminosity Function

M_{1450} Bin Center (mag)	$\langle M_{1450}\rangle$[a] (mag)	Φ (10^{-8} Mpc^{-3} mag^{-1})	$N_{\rm QSO}$
SDSS			
−28.5	−28.45	$0.008^{+0.011}_{-0.005}$	2
−27.5	−27.33	$0.20^{+0.04}_{-0.03}$	41
−26.5	−26.46	0.93 ± 0.07	169
−25.5	−25.70	4.3 ± 0.5	102
−24.5	−24.72	$0.4^{+0.3}_{-0.2}$	4
NDWFS+DLS			
−25.5	−25.37	24^{+13}_{-9}	7
−24.5	−24.71	$8.8^{+8.5}_{-4.8}$	3
−23.5	−23.47	143^{+77}_{-53}	7
−22.5	−22.61	307^{+208}_{-133}	5
−21.5	−21.61	434^{+572}_{-280}	2

Note. [a] Mean magnitude of the QSOs in each bin.

space densities of the binned QLF from SDSS and our QSOs. We compute uncertainties for the bins with small numbers of QSOs (<50) using Gehrels (1986). Our improved spectroscopic completeness lowers the space density of the lowest luminosity bin by a factor of 12 or approximately 1.2σ relative to the poorly constrained value presented in Paper I.

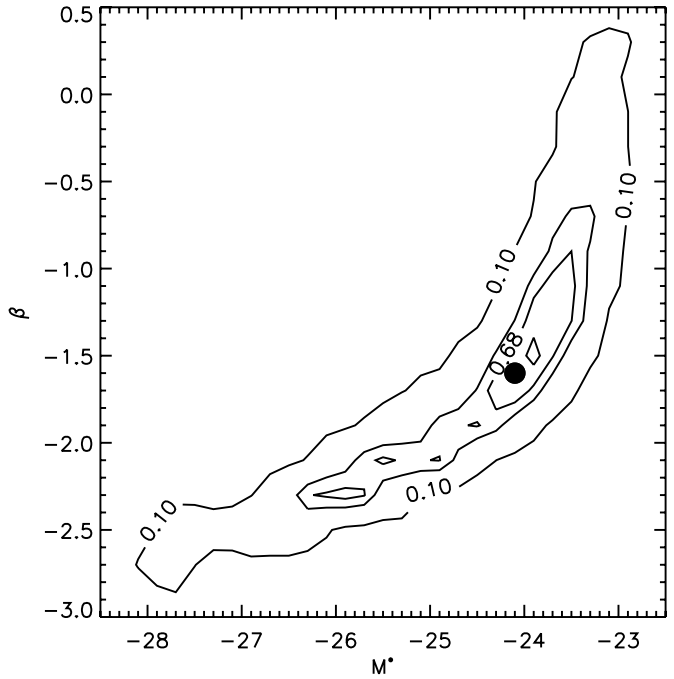

Figure 4. We show the probability density of the faint-end slope, β, vs. break absolute magnitude, M^*, based on 10,000 Monte Carlo simulations of our binned QLF. Contour levels are 10%, 50%, 68%, and 90% of the peak density. The best-fit parameters to the real QLF is plotted with a filled circle.

5. THE SHAPE OF THE QLF

We fit the QLF using the STY maximum likelihood method (Efstathiou et al. 1988). Initially we fit a single power-law function, which was the best-fit function found in Paper I. The likelihood is maximized for a single power law with $\alpha = -3.3 \pm 0.1$ at 68% confidence, ± 0.2 at 90% confidence, and ± 0.3 at 99% confidence. This value is effectively a measure of the bright-end slope of the QLF and is consistent with Croom et al. (2004) for the $0.4 < z < 2.1$ range.

Similarly, we measured the slope of a single power law at the faint end, using only quasars fainter than $M_{1450} = -24$. The likelihood is maximized with $\beta = -1.6 \pm 0.2$ at 68% confidence, +0.3, −0.4 at 90% confidence, and +0.4, −0.6 at 99% confidence.

We also fit the binned QLF to a double power-law function,

$$\Phi(M) = \frac{\Phi(M^*)}{10^{0.4(\alpha+1)(M-M^*)} + 10^{0.4(\beta+1)(M-M^*)}}, \qquad (1)$$

omitting the outlying SDSS point at $M_{1450} = -24.5$. The resultant curve is plotted in Figure 3 with a solid black line. The shaded region represents the 1σ uncertainties, which we determine by simulating 10,000 random QLFs based on our binned $\Phi(M)$ measurements and their associated errors. The best-fit parameters are $\Phi^* = \Phi(M^*) = 1.3^{+1.8}_{-0.2} \times 10^{-6}$ Mpc^{-3} mag^{-1}, $\alpha = -3.3 \pm 0.2$, $\beta = -1.6^{+0.8}_{-0.6}$, and $M^* = -24.1^{+0.7}_{-1.9}$ ($\chi^2 = 1.12$). Figure 4 shows the distribution of β versus M^* from our simulations, with the best-fit value overplotted (filled circle).

The results from Ikeda et al. (2011) are overplotted in Figure 3 as blue squares. The dot-dashed line is their best-fit double power law. While our newly measured faint-end slope agrees with their value of $\beta = -1.67^{+0.11}_{-0.17}$, our normalization ($\Phi^*$) is higher by a factor of four and our break luminosity is fainter by 0.3 mag.

We overplot in Figure 3 the QLF at $z \sim 3$ from Siana et al. (2008), who selected QSOs using infrared and optical photometry in the SWIRE Legacy Survey (Lonsdale et al. 2003). The dashed line is their best-fit QLF to only the SWIRE data, while the dotted lines are fits to their SDSS+SWIRE QLF. Both the bright- and faint-end slopes are comparable at $z \sim 3$ and $z \sim 4$. The most striking evolution occurs at M^* which, while poorly constrained, is 1–1.5 mag fainter at $z \sim 4$ than at $z \sim 3$, according to our fit.

This is apparently at odds with the so-called cosmic downsizing where the space density of AGNs peaks at different times for different luminosities. Low-luminosity AGNs are more abundant at low redshifts and the space density of high-luminosity AGNs peaks at earlier times. This is seen in the evolution of the X-ray QLF (e.g., Barger et al. 2005) and in the optical at lower redshifts (e.g., Croom et al. 2009). However, this has not been well explored past the peak of the quasar epoch ($z \sim 2.5$–3). Based on QSOs in SDSS Stripe82, 2 mag deeper than Richards et al. (2006), Jiang et al. (2006) did not see evidence for AGN downsizing at these redshifts.

6. THE CONTRIBUTION OF QUASARS TO THE UV RADIATION FIELD AT $z \sim 4$

Following the same calculation as in Paper I, but using the new parameters of the double power-law QLF, we calculate the emissivity of quasars at 1450 Å to be $\epsilon_{1450} = 3.5^{+14.1}_{-2.4} \times 10^{25}$ erg s^{-1} Hz^{-1} Mpc^{-3}, ~50% of our earlier result. Siana et al. (2008) compute the specific luminosity density from QSOs at $z \sim 3.2$ to be $\epsilon_{1450} = 5.1 \times 10^{24}$ erg s^{-1} Hz^{-1} Mpc^{-3}. This is a factor of ~7 lower than what we compute at $z \sim 4$.

Following the formalism of Madau et al. (1999), $\dot{N}_{\rm IGM} = 2.4 \times 10^{51}$ s^{-1} ionizing photons are needed to ionize the IGM at $z = 4.15$ (the median redshift of our survey). Our parameterized QLF produces $\dot{N}_{\rm QSO} = 1.5^{+6.0}_{-1.0} \times 10^{51}$ s^{-1} or ~60% ± 40% of the photons ionizing the IGM. Siana et al. (2008) argue that at $z \sim 3$ QSOs contribute just under half the needed photons to ionize the IGM, which is roughly consistent with our result. In addition, Vanzella et al. (2010) find that $z \sim 4$ LBGs in the Great Observatories Origins Deep Surveys (Giavalisco et al. 2004) account for <20% of the photons needed to ionize the IGM, leaving QSOs as the likely dominant ionizing source at this redshift.

We thank Gordon Richards for useful discussions on combining the SDSS and our QLFs, and Meg Urry for helpful comments. We are grateful to the staff of W. M. Keck observatory for their assistance during our observing runs. This work was supported in part by the NSF grants AST-0407448 and AST-0909182, and by the Ajax foundation. The work of D.S. was carried out at Jet Propulsion Laboratory, California Institute of Technology, under a contract with NASA. The research activities of A.D. and B.T.J. are supported by the NSF through its funding of the NOAO, which is operated by the Association of Universities for Research in Astronomy, Inc. under a cooperative agreement with the NSF. This work makes use of image data from the NDWFS and the DLS as distributed by the NOAO Science Archive. K.S.L. gratefully acknowledges the generous support of Gilbert and Jaylee Mead for their namesake fellowship.

REFERENCES

Barger, A. J., Cowie, L. L., Mushotzky, R. F., Yang, Y., Wang, W., Steffen, A. T., & Capak, P. 2005, AJ, 129, 578
Bertin, E., & Arnouts, S. 1996, A&AS, 117, 393
Cristiani, S., & Vio, R. 1990, A&A, 227, 385
Croom, S. M., Smith, R. J., Boyle, B. J., Shanks, T., Miller, L., Outram, P. J., & Loaring, N. S. 2004, MNRAS, 349, 1397
Croom, S. M., et al. 2009, MNRAS, 399, 1755
Downes, R. A., et al. 2004, AJ, 127, 2838
Efstathiou, G., Ellis, R. S., & Peterson, B. A. 1988, MNRAS, 232, 431
Fontanot, F., Cristiani, S., Monaco, P., Nonino, M., Vanzella, E., Brandt, W. N., Grazian, A., & Mao, J. 2007, A&A, 461, 39
Gehrels, N. 1986, ApJ, 303, 336
Giavalisco, M., et al. 2004, ApJ, 600, L93
Glikman, E., Bogosavljević, M., Djorgovski, S. G., Stern, D., Dey, A., Jannuzi, B. T., & Mahabal, A. 2010, ApJ, 710, 1498
Glikman, E., Djorgovski, S. G., Stern, D., Bogosavljević, M., & Mahabal, A. 2007, ApJ, 663, L73
Haiman, Z., Abel, T., & Madau, P. 2001, ApJ, 551, 599
Hunt, M. P., Steidel, C. C., Adelberger, K. L., & Shapley, A. E. 2004, ApJ, 605, 625
Ikeda, H., et al. 2011, ApJ, 728, L25
Jannuzi, B. T., & Dey, A. 1999, in ASP Conf. Ser. 191, Photometric Redshifts and the Detection of High Redshift Galaxies, ed. R. Weymann et al. (San Francisco, CA: ASP), 111
Jiang, L., et al. 2006, AJ, 131, 2788
Lee, K., et al. 2010, arXiv:1009.3022
Lonsdale, C. J., et al. 2003, PASP, 115, 897
Madau, P., Haardt, F., & Rees, M. J. 1999, ApJ, 514, 648
Page, M. J., & Carrera, F. J. 2000, MNRAS, 311, 433
Pei, Y. C. 1995, ApJ, 438, 623
Richards, G. T., et al. 2002, AJ, 123, 2945
Richards, G. T., et al. 2006, AJ, 131, 2766
Shankar, F., & Mathur, S. 2007, ApJ, 660, 1051
Siana, B., et al. 2008, ApJ, 675, 49
Steidel, C. C., Adelberger, K. L., Giavalisco, M., Dickinson, M., & Pettini, M. 1999, ApJ, 519, 1
Vanzella, E., et al. 2010, ApJ, 725, 1011
Wittman, D. E., Margoniner, V., Tyson, J. A., Cohen, J. G., Becker, A., & Dell'Antonio, I. P. 2002, Proc. SPIE, 4836, 73
Wolf, C., Wisotzki, L., Borch, A., Dye, S., Kleinheinrich, M., & Meisenheimer, K. 2003, A&A, 408, 499
Wyithe, J. S. B., & Loeb, A. 2003, ApJ, 586, 693